Donor's age and replicative senescence favour the *in-vitro* mineralization potential of human fibroblasts.

Federica Boraldi*, Angelica Bartolomeo*, Caterina Di Bari, Andrea Cocconi, Daniela Quaglino

Department of Life Sciences, University of Modena and Reggio Emilia, Modena, Italy

* Equally contributed to the paper

Address for correspondence:

Prof. Daniela Quaglino

Department of Life Sciences

University of Modena and Reggio Emilia,

Via Campi 287 - 41125 Modena (Italy)

E-mail daniela.quaglino@unimore.it

Abstract

Aberrant mineralization of soft connective tissues (ectopic calcification) may occur as a frequent age-related complication. Still, it remains unclear the role of mesenchymal cell donor's age and of replicative senescence on ectopic calcification. Therefore, the ability of cells to deposit *in-vitro* hydroxyapatite crystals and the expression of progressive ankylosis protein homolog (ANKH), ectonucleotide pyrophosphatase/phosphodiesterase 1 (ENPP1), tissue non specific alkaline phosphatase (TNAP) and osteopontin (OPN) have been evaluated in human dermal fibroblasts derived from neonatal (nHDF) and adult (aHDF) donors (*ex-vivo* ageing model) or at low and high cumulative population doublings (CPD) up to replicative senescence (*in-vitro* ageing model). This study demonstrates that: 1) replicative senescence favours hydroxyapatite formation in cultured fibroblasts; 2) donor's age acts as a major modulator of the mineralizing potential of HDF, since nHDF are less prone than aHDF to induce calcification; 3) donor's age and replicative senescence play in concert synergistically increasing the calcification process; 4) the ANKH+ENPP1/TNAP ratio, being crucial for pyrophosphate/inorganic phosphate balance, is greatly influenced by donor's age, as well as by replicative senescence, and regulates mineral deposition; 5) OPN is only modulated by replicative senescence.

1. Introduction

Ageing connective tissues undergo progressive morphological, biochemical and functional modifications contributing to fibrosis and/or to loss of elasticity, thus reducing the ability to respond to mechanical stress and increasing the risk of age-related diseases. Within this context, vascular ageing and a number of pathologic conditions (i.e. diabetes, end-stage renal disease, inflammation and oxidative stress) are characterized by ectopic calcification that is considered a strong predictor of cardiovascular events (Giachelli et al., 2005; Shao et al., 2010). Although frequently observed in the vascular system and described since the 19th century (Burger, 1947), mineral deposition may occur also in valves, cartilage, tendons, skeletal muscle and skin (Selye, 1962; Kirsch, 2012; Siddiqui and Altorok, 2015; Endo, 2015). However, it has to be mentioned that ectopic calcification, even within a tissue, is not a diffuse process, but it is limited to specific areas, consistent with the complexity of cellular and/or extracellular factors locally acting as promoters or inhibitors of hydroxyapatite deposition. Moreover, mesenchymal cells, producing and secreting the majority of extracellular components, modulate connective tissue homeostasis, playing a key role in several pathologic conditions and in age-related complications as those due to aberrant mineralization (Ronchetti et al., 2013). Despite the life-threatening consequences of ectopic calcification, most studies have mainly investigated vascular smooth muscle cells (VSMC) and only few data are available on other mesenchymal cells and on their role in the age-related susceptibility of connective tissues to mineral deposition (Ronchetti et al., 2013). It has been reported that vascular calcification is associated to cellular senescence suggesting that this behaviour is limited to VSMC (Burton et al., 2010). The observation that altered phosphate regulation can be responsible for the mineralization of soft connective tissues in premature ageing syndromes (MacKenzie and MacRae, 2011; Shanahan, 2013), further sustains the link between ageing and ectopic calcification and underlines the importance of the phosphate circuitry in these events.

Aim of the present study was to investigate whether human dermal fibroblast cell lines, derived either from neonatal or adult donors and cultured upon senescence, have a different ability to form a calcified matrix and to exhibit changes in the expression of proteins, that, being related to inorganic pyrophosphate/phosphate (PPi/Pi) balance, have been demonstrated to regulate vascular calcification (Giachelli et al., 2005). In particular, Pi acts as a signalling molecule and a necessary source for hydroxyapatite formation, whereas PPi acts as a potent inhibitor, but it can be quickly and efficiently hydrolysed by tissue-non specific alkaline phosphatase (TNAP), releasing Pi and loosing its inhibitor

activity. The levels of PPi and Pi are therefore tightly regulated by TNAP, but also by other molecules such as progressive ankylosis protein homolog (ANKH) and pyrophosphatase/phosphodiesterase 1 (ENPP1) (Rodriguez et al., 2012). The first is a multi-pass trans-membrane protein mediating intracellular to extracellular channelling of PPi (Hakim et al., 1984; Ho et al., 2000), whereas the latter generates PPi from nucleoside triphosphates (Terkeltaub et al., 1994; Johnson et al., 1999). Therefore, changes in PPi/Pi ratio can induce or inhibit calcium-phosphate salt deposition. In addition, phosphate availability can also modulate osteopontin (OPN) expression, an inhibitor of hydroxyapatite crystal growth.

We have already demonstrated that human dermal fibroblasts from donors of different age (Boraldi et al., 2003) or cultured *in-vitro* for several passages upon senescence represent useful and informative models to investigate age-related phenotypic changes (Boraldi et al., 2010). Therefore, we have used both the *ex-vivo* and *in-vitro* ageing models to better understand whether fibroblasts cultured in standard or in calcifying media may exhibit an age-dependent increased susceptibility to pro-mineralizing factors, especially focusing on those related to the phosphate circuitry.

2. Methods

2.1 Cell culture

Neonatal (nHDF) (Cat # C-004-5C) and adult human dermal fibroblasts (aHDF) (Cat # C-013-5C) were purchased from ThermoFisher Scientific (Waltham, MA,USA)

Cells were grown in DMEM supplemented with 10% foetal bovine serum (FBS) (Gibco-Thermo Fisher Scientific) according to standard procedures (Quaglino et al., 2000). Initially, cell lines were sub-cultured weekly, whereas slow growing cultures were sub-cultured biweekly. The number of population doublings (PD) was calculated using the formula (van der Loo et al., 1998):

PD= ln (number of cells harvested) - ln (number of cells seeded) / ln2

The calculated population doubling increase was then added to the previous population doubling value, to yield the cumulative population doubling level (CPD). The end of the replicative lifespan was defined by failure of cell population to double after 20 days in culture despite 3 changes/week of the culture medium.

In this study, we have analysed cell lines at low CPD (i.e. CPD values between 4-6 in both nHDF and aHDF) and at high CPD (i.e. CPD values between 61-64 and 45-49 for nHDF and aHDF, respectively).

Cells were always grown in parallel and regularly observed under the inverted light microscope.

2.2 β-galactosidase (β-gal) activity

The fluorogenic substrate $C_{12}FDG$ (ImaGene Green) (Thermo Fisher Scientific) was used in the presence or absence of chloroquine, an inhibitor of endogenous β-gal. $C_{12}FDG$ is a membrane permeable non-fluorescent substrate for β-gal, which, after hydrolysis of the galactosyl residues, emits a green fluorescence that remains confined within the cell. Fibroblasts were plated in 35 mm dishes at the density of 1.2 X 10^5 cells. After 2 days from seeding, the majority of cells were still in a proliferative state. Therefore, some dishes were pre-treated with 300 mM chloroquine for 90 min at 37 °C. All dishes were then incubated with 300 mM of $C_{12}FDG$ for 1 h. Cells were washed in ice-cold PBS, detached with trypsin and centrifuged. The obtained pellets were re-suspended in 300 ml of PBS and ten thousand events were analysed. Fluorescence was measured at the emission wavelength of 520 nm. Experiments were conducted three times in duplicate.

2.3 In-vitro mineralization assay

Fibroblasts were routinely grown in standard medium supplemented with 10% FBS up to confluence (DMEM). For mineralization experiments, confluent cells were maintained in culture with calcifying medium (CM) comprised of DMEM supplemented with ascorbic acid (50µg/ml) (Sigma, St. Louis, MO); β-glycerol phosphate (10mM) (Sigma) and dexamethasone (10nM) (Sigma) (Boraldi et al., 2013; 2014). After 10-20-30 days, mineralization was assessed by phosphate staining in the extracellular matrix with von Kossa method. Areas of mineralization were quantified on digital images by Image software. Experiments were conducted three times in triplicate.

2.4 Tissue-non specific alkaline phosphatase (TNAP) activity

TNAP activity was measured spectrophotometrically at 405nm on nHDF and aHDF at both low and high CPD cultured in DMEM or in CM and values of optical density were related to $1x10^6$ cells. Experiments were performed three times in triplicate.

2.5 Western blot

Cells were washed several times with phosphate-buffered saline and homogenized in RIPA buffer (50 mM Tris, pH 7.5, 0.1% Nonidet P-40, 0.1% deoxycholate, 150 mM NaCl,

and 4 mM EDTA) (Sigma) in the presence of protease inhibitors (Sigma). Cellular lysates were centrifuged at 15,000 rpm for 20 min to clear cell debris, and supernatants were collected and stored at -80°C until analysis. Protein concentration in the cellular extracts was determined using the Bradford method (Bradford, 1976). Protein extracts (40 mg proteins/lane) for each cell line and for each culture condition were separated by electrophoresis on 10-lane 10% polyacrylamide gels under reducing conditions and transferred onto nitrocellulose membranes. Membranes were blocked in TBS + 0.1% Tween 20 (TBST) + 5% non-fat dry milk for 1 h at room temperature. Primary antibodies were diluted in TBST + 2,5% non-fat dry milk as follows: (i) progressive ankylosis protein homolog (ANKH) 1:1000 (rabbit polyclonal, Santa Cruz Biotechnology, Dallas, TX); (ii) ectonucleotide pyrophosphatase/phosphodiesterase 1 (ENPP1) 1:500 (rabbit polyclonal, Santa Cruz Biotechnology); (iii) osteopontin (OPN) 1:600 (rabbit polyclonal, Santa Cruz Biotechnology). Membranes were incubated with primary antibodies overnight. Appropriate horseradish peroxidase (HRP)-conjugated secondary antibodies (Abcam, Cambridge, UK, diluted 1:5000) were used after 3 washes of membranes in TBST. Western blots were visualized using Super Signal West Pico (Pierce-Thermo Fisher Scientific) according to manufacturer's protocols. Experiments were performed two times in triplicate for each cell line and culture condition.

2.6 *Data analysis*

Statistical analysis was performed using GraphPad Prism software, version 5.01 for MAC (GraphPad Software, San Diego, CA, USA). Data sets were compared by ANOVA or by non-parametric analysis of Mann–Whitney test. P values less than 0.05 were considered statistically significant.

3. Results

3.1 Morphology, cell proliferation and β-gal activity.

Independently from donor's age, both neonatal and adult fibroblasts at low CPD exhibited the elongated shape typical of mesenchymal cells (Fig. 1A and B), but nHDF reached confluence in a shorter time compared to aHDF (data not shown). At high CPD, when cells were close to replicative senescence, all fibroblasts appeared larger with abundant vacuolated cytoplasm leaving numerous empty spaces on the plate surface even after several days of culture (Fig. 1C and D). Replicative senescence was confirmed by

increased β-gal activity. The number of β-gal positive cells, as revealed by the shift of fluorescence intensity values, rose progressively with increased CPD (Fig. 1E and 1F). To be noted that the lifespan of cultured nHDF and aHDF, represented by the maximum number of CPD obtained *in-vitro,* was lower in aHDF (48 CPD) compared to nHDF (64 CPD) (*p<0.05).

3.2 Mineral deposition in ex-vivo and in in-vitro ageing models

Neonatal and adult fibroblasts, at both low and high CPD, were cultured in parallel in standard and in pro-calcifying media.

As expected, in standard medium all fibroblasts never exhibited mineral deposition (Fig. 2).

Calcification started to be clearly visible around 20 days of culture in pro-calcifying medium, however the extent of mineralization was highly variable depending both on donor's age and on the number of CPD. In particular, few small precipitates were observed in nHDF at low CPD, whereas their number and size progressively and significantly increased at higher CPD (Fig. 3A). At 30 days of culture in CM, the area covered by mineral deposits on the cellular monolayer was more than 20% and less than 4% at high and low CPD, respectively (Fig. 3B). A similar trend was observed also in aHDF (Fig. 4A), however the amount of mineral deposits was markedly increased at all times compared to nHDF (Fig. 3 and 4). At 30 days of culture in CM, the mineralized area measured in aHDF at low CPD was approximately 20% of the cellular monolayer (Fig. 4B), whereas adult fibroblasts at high CPD were almost completely mineralized (99%) (Fig. 4B).

3.3 TNAP activity

Since mineral deposition is, at least in part, due to TNAP, the enzyme activity was measured in all experimental conditions (Fig. 5). TNAP activity significantly increased over time in cells cultured in CM and values were higher compared to fibroblasts grown in standard medium. Although there was not a direct correlation between enzyme activity and the extent of mineralization, nevertheless, in the same cell line, values were significantly increased in fibroblasts at high compared to low CPD (Fig. 5A and B). Moreover, starting from the 20th day of culture in CM, TNAP activity, at low CPD, was significantly higher in aHDF than in nHDF (p<0.05), whereas at high CPD differences were visible already from 10th day of culture in CM (p<0.01).

3.4 Proteins expression by Western blot.

Increased TNAP activity is necessary, but non sufficient, for mineral deposition. Therefore, ANKH, ENPP1 and OPN expression have been quantified by Western blot, since the first two proteins are directly involved in PPi/Pi balance, and OPN is regulated by changes in Pi availability (Fig. 6).

In order to assess fibroblasts' response to pro-calcifying factors and the influence of ageing *per se,* protein expression has been evaluated in CM and in DMEM, respectively.

The amount of ANKH in nHDF was not modified by *in-vitro* senescence, neither by the presence of calcifying factors. By contrast, in aHDF, the expression of ANKH was influenced by *in-vitro* senescence, since values increased in cells cultured in DMEM at high CPD. Moreover, at low CPD, ANKH expression in standard medium was significantly reduced in aHDF compared to nHDF, indicating an effect of donor's age. When aHDF were cultured in a mineralizing environment, ANKH expression increased only at high CPD.

When cells were cultured in DMEM, ENPP1 expression was significantly increased at high compared to low CPD in nHDF. By contrast, in CM, ENPP1 was up-regulated at low CPD, whereas it was unchanged at higher CPD. Interestingly, the very low levels of protein expression observed in aHDF, both at low and high CPD in DMEM, appeared to be progressively up-regulated in CM.

In DMEM, OPN was similarly expressed in both nHDF and aHDF at low CPD and was up-regulated by replicative senescence. OPN expression remained unmodified in the presence of CM.

3.5 Proportional contribution of proteins regulating PPi levels

ANKH, ENPP1 and TNAP play in concert regulating intra-and extracellular PPi levels. In order to better evaluate the occurrence of a protein expression shift towards a pro-mineralizing condition, it is important to look at the proportional contribution of each protein. The 100% stacked column chart has been applied to further highlight the significance of results. In particular, we have compared the percentage of each protein expression in two representative experimental conditions [i.e. a condition never associated to mineralization (DMEM) and a condition associated to a variable amount of calcification (30 days in CM)] (Fig. 7). If the ANKH+ENPP1/TNAP ratio in nHDF at low CPD cultured in DMEM is normalized to 100%, values decreased to 87% and 75% in nHDF in CM at low

and high CPD, respectively, and to 21% and 15% in aHDF in CM at low and high CPD, respectively.

4. Discussion

Pathologic calcification of soft connective tissues represents a complication contributing to age-related tissue dysfunction, nevertheless only few studies have investigated whether the ageing phenotype of mesenchymal cells is associated or not with an increased response to pro-calcifying stimuli (Mackenzie and MacRae, 2011). Data obtained so far, focusing on vascular smooth muscle cells, lead to the hypothesis that the increased susceptibility to mineralizing stimuli of senescent cells may be peculiar of this cell type (Burton et al., 2010).

Therefore, we have compared the behaviour of two fibroblast cell lines (*ex-vivo* ageing model) derived from neonatal and from adult individuals, the first being minimally influenced by exogenous and/or by the extracellular environment, the latter having experienced several stresses contributing to epigenetic modifications and to age-related changes (Aviv, 2004). Nevertheless, when cells are placed in culture, independently from the donor's age, they may undergo a phenotypic selection. Therefore, as we have already demonstrated, fibroblasts cultured *in-vitro* for several passages, upon reaching replicative senescence, may represent a condition (*in-vitro* ageing model) mimicking more closely changes occurring during *in-vivo* ageing, at least for a number of parameters (Boraldi et al 2010).

The use of these models allows to better understand if donor's age and/or replicative senescence influence the mineralizing potential of mesenchymal cells other than vascular smooth muscle cells (i.e. dermal fibroblasts).

We have observed an inverse relationship between donor's age and proliferative lifespan in agreement with Martin and co-workers (1970), whereas other studies (Cristofalo et al., 1998; Boraldi et al., 2010) failed to find this correlation. This discrepancy may be due to the fact that in the present study we have compared fibroblasts from neonatal donors with those from adult individuals, whereas in other studies fibroblasts from adult and old donors were compared with those from young subjects. Consistently, our laboratory demonstrated that in the skin equivalent model, best results, in terms of matrix production and cell proliferation, were obtained with neonatal fibroblasts compared to young or adult cells (Croce et al., 2004). Taken together these results indicate that fibroblasts loose their juvenile behaviour quite early, even when cells are placed in optimum culture conditions. It

may be suggested that in addition to intrinsic (i.e. genetic) factors, extrinsic influences (i.e life style and exposure to environmental noxae) may trigger, for instance, genome instability, telomere attrition and loss of proteostasis acting on proliferative lifespan and on the capacity of these cells to secrete extracellular matrix proteins.

Moreover, in agreement with previous data (Kurz et al., 2000; Maier et al., 2007; Boraldi et al., 2010), nHDF and aHDF are characterized by the presence, already at low CPD, of β-gal positive cells, indicating that also *in-vitro* senescent and quiescent cells coexist. Morphological changes and increased β-gal activity observed in both cell lines were associated with reduced growth capacity and therefore with increased CPD, however the replicative lifespan was mainly influenced by donor's age.

To induce *in-vitro* calcification, cells were cultured in CM at both low and high CPD. This medium is necessary since mesenchymal cells, in standard culture conditions, are not able to promote mineralization due to the presence of serum inhibiting molecules as fetuin (Buranasinsup et al., 2006; Boraldi et al., 2013). The amount of hydroxyapatite deposition (Boraldi et al., 2014) depends on time in culture (up to 30 days in CM), donor's age (neonatal and adult) and cellular senescence (low and high CPD), in agreement with the *in-vivo* prevalent occurrence of calcification in ageing soft connective tissues.

Although mineral deposition is a very complex process involving numerous promoting and inhibiting factors, it has been observed in VSMC that phosphate availability plays a key role in controlling pathologic calcification (Giachelli, 2005).

Within this context, TNAP is an ectoenzyme capable to dephosphorylate a broad range of molecules (i.e phosphoproteins, PPi, β-glycerophosphate) favouring mineral deposition and crystal growth (Millàn, 2006). In both the *ex-vivo* and *in-vitro* ageing models, there was a progressive increase of TNAP activity, even if nHDF exhibited values significantly lower than aHDF. As already demonstrated by Mendes and co-workers (2004), there is not a direct correspondence between TNAP activity and the amount of deposited mineralized matrix, since TNAP *per se* is necessary, but not sufficient to induce mineral deposition (Boraldi et al., 2013) and a threshold PPi/Pi ratio must be reached. After 30 days of culture in CM, nHDF were always less susceptible to pro-calcified factors in comparison with aHDF. Cells from neonatal donors were characterized by: high levels of ENPP1, stable ANKH expression and only a moderate increase of TNAP activity. The resistance to calcification seems to be associated to the high expression of ENPP1 triggering the formation of PPi capable to inhibit hydroxyapatite deposition. On the contrary, aHDF exhibited increased ANKH and ENPP1, although ENPP1 never reached the levels of

nHDF. These changes, associated with a strong increase of TNAP activity, may explain, at least in part, the abundance of hydroxyapatite in aHDF cultures. In fact, although ENPP1 up-regulation can increase PPi production, this inhibitor is actively hydrolysed by the huge increase of TNAP, thus releasing Pi that is responsible for the extensive mineral deposition revealed by von Kossa staining.

The concerted action of TNAP, ANKH and ENPP1 regulates PPi levels, therefore when ANKH and ENPP1 overcome TNAP (as in HDF cultured in DMEM) hydroxyapatite deposition is never observed, by contrast, when TNAP prevails on ANKH and ENPP1 (as in aHDF at high CPD in CM) there is an almost complete mineralization of the cellular monolayer. These effects are mainly dependent on donor's age and are further modified by replicative senescence.

Several reports have suggested that, in VSMC, osteopontin acts as an inhibitor of calcification, being calcium-dependent and associated with apatite crystal growing (Wada et al., 1999). Although it has been demonstrated that there is a tight link between osteopontin expression and phosphate levels (Beck et al., 2000), this protein does not interfere with TNAP activity or with phosphorus levels (Wada et al., 1999). Therefore, we have investigated the expression of this protein in *ex-vivo* and *in-vitro* ageing models and in the presence of CM in order to evaluate if the expression of osteopontin can be modulated by a medium providing phosphate-releasing substrates. We have found that replicative senescence, in both cell lines, induced increased OPN levels in agreement with previous findings in senescent fibroblasts (Pazolli et al., 2009; Liu et al., 2012), but OPN expression was never modified by the presence of CM. These data further sustain the complex role of this multifunctional matri-cellular protein that seems to act as a regulator of mineral deposition mainly in conditions of injury and disease (Giachelli et al., 2005), whereas its role as an endogenous natural inhibitor is still questionable (Lomashvili et al., 2004).

5. Conclusion

In summary, this study highlights, for the first time, that: 1) replicative senescence favours hydroxyapatite formation in fibroblasts as shown in VSMC (Burton, 2010), demonstrating that this behaviour is not limited to a specific mesenchymal cell type; 2) donor's age acts as a major modulator of the mineralizing potential of HDF, since nHDF are less prone than aHDF to induce calcification in all examined experimental conditions; 3) donor's age and

replicative senescence play in concert synergistically increasing the calcification process; 4) the ANKH+ENPP1/TNAP ratio is crucial for mineral deposition and is dramatically influenced by donor's age but also by replicative senescence; 5) OPN is only modulated by replicative senescence (Table 1).

In the light of these results, it could be suggested that ageing human fibroblasts may have a strong mineralizing potential and this may be also the consequence of epigenetic changes that are known to accumulate throughout life (Robert et al., 2009) and that may trigger the reduced capacity of fibroblasts to inhibit the calcification process.

Conflict of interest

No conflicts of interest are declared

Figure captions

Fig. 1. Cell morphology by light microscopy (A-D) and β-galactosidase activity (β-gal) by flow cytometry (E-F). Evaluations were performed in neonatal (nHDF) and adult human (aHDF) dermal fibroblasts, at both low and high CPD, cultured in standard medium. When cells reached replicative senescence, they exhibited an enlarged and irregular shape as well as several vacuoles (C,D). A representative experiment of β-gal measurement is reported in panel E. Cells pre-treated with chloroquine (-) were used as a negative control, thus indicating that enzyme activity was only of intracellular origin. The number of positive cells is revealed by the shift of fluorescence intensity values on the abscissa. The effect of *ex-vivo* ageing *(*nHDF vs aHDF*)* and *in-vitro* ageing (different CPD within the same cell line) on β-gal are shown in panel F. Data are expressed as mean values ± SEM and compared with those obtained in nHDF at 5 CPD that was set at one. ***$p<0.0001$ 5 CPD vs other CPD in the same cell line; °°$p<0.001$ nHDF vs aHDF at comparable CPD

Fig. 2. von Kossa staining in standard conditions. Neonatal (nHDF) and adult (aHDF) human dermal fibroblasts, at both low and high CPD, were cultured in DMEM. Absence of mineral deposition was evident after von Kossa staining. Bar: 120 μm.

Fig. 3. *In-vitro* calcification assay. (A) Neonatal human dermal fibroblasts (nHDF), at both low (L) and high (H) CPD, were cultured in calcifying medium for 10-20-30 days (d). Hydroxyapatite deposition (arrows) was assessed by phosphate staining in the extracellular matrix with the von Kossa method. Bar: 120 μm. (B) Histogram quantifies the amount of calcified areas at different culture time points. Data are expressed as mean values ± SEM. *$p< 0.05$; **$p< 0.01$

Fig. 4. *In-vitro* calcification assay. A) Adult human dermal fibroblasts (aHDF), at both low (L) and high (H) CPD, were cultured in calcifying medium for 10-20-30 days (d). Hydroxyapatite deposition (arrows) was assessed by phosphate staining in the extracellular matrix with the von Kossa method. Bar: 120 μm. (B) Histogram quantifies the amount of calcified areas at different culture time points. Data are expressed as mean values ± SEM. **$p< 0.01$; ***$p< 0.001$

Fig. 5. TNAP activity. Enzyme activity was measured in neonatal (nHDF) (A) and adult (aHDF) (B) human dermal fibroblasts, at both low (L) and high (H) CPD. Fibroblasts were cultured until confluence with standard medium (DMEM) and then with calcifying media (CM) for 10-20-30 days (d). TNAP activity for $1X10^6$ cells is expressed as mean values ± SEM. The time-dependent trend of TNAP activity in both cells lines is shown in graphs. *p< 0.05; **p< 0.01; ***p< 0.001

Fig. 6. ANKH, ENPP1 and OPN expression by Western blot. Neonatal (nHDF) and adult (aHDF) human dermal fibroblasts were cultured at confluence in standard medium (DMEM) and for 10, 20 and 30 days (d) in calcifying medium (CM) at both low and high CPD.

In nHDF/aHDF-DMEM panels, each protein expression is compared with values of the same protein in nHDF at low CPD which has been set at 1 in order to assess age-related changes independently from the presence of pro-calcifying factors.

In nHDF-DMEM/CM and aHDF-DMEM/CM panels, each protein expression is compared with values of the same protein in nHDF and aHDF at low CPD in DMEM, respectively, which has been set at 1 in order to evaluate, for each cell line, the time-dependent influence of CM on protein expression also in relation to increased CPD (i.e. replicative senescence). On top of each panel a representative Western blot is shown.

Data are expressed as mean values ± SEM; * p<0.05; ** p<0.01 high CPD *vs* low CPD in the same cell line; § p<0.05; §§ p<0.01 aHDF *vs* nHDF at the same CPD; # p<0.05; ## p<0.01 CM *vs* DMEM.

Tables in the right side of the figure show changes of protein expression in nHDF and in aHDF cultured in DMEM and CM at low and high CPD. All experimental conditions, for each protein, are compared with value of nHDF at low CPD in DMEM which has been set at 1 in order to evaluate, as a trend, the combined influence of CM, donor's age and replicative senescence.

Fig. 7. The 100% stacked column charts are used to graphically visualize the percentage contribution of ANKH, ENPP1 and TNAP in neonatal (nHDF) and adult (aHDF) human dermal fibroblasts cultured in calcifying medium (CM) for 30 days at both low and high CPD in comparison with nHDF at low CPD cultured in DMEM.

References

Aviv A. Telomeres and human aging: facts and fibs. Sci Aging Knowledge Environ. 2004; 51: 43.

Beck GR Jr, Zerler B, Moran E. Phosphate is a specific signal for induction of osteopontin gene expression. Proc Natl Acad Sci U S A. 2000;97:8352-8357.

Boraldi F, Annovi G, Bartolomeo A, Quaglino D. Fibroblasts from patients affected by Pseudoxanthoma elasticum exhibit an altered PPi metabolism and are more responsive to pro-calcifying stimuli. J Dermatol Sci. 2014;74:72-80.

Boraldi F, Annovi G, Tiozzo R, Sommer P, Quaglino D. Comparison of ex vivo and in vitro human fibroblast ageing models. Mech Ageing Dev. 2010;131:625-635.

Boraldi F, Annovi G, Vermeer C, et al. Matrix gla protein and alkaline phosphatase are differently modulated in human dermal fibroblasts from PXE patients and controls. J Invest Dermatol. 2013;133:946-954.

Boraldi F, Bini L, Liberatori S, Armini A, Pallini V, Tiozzo R, Pasquali-Ronchetti I, Quaglino D. Proteome analysis of dermal fibroblasts cultured in vitro from human healthy subjects of different ages. Proteomics. 2003;3:917-929.

Bradford MM. A rapid and sensitive method for the quantitation of microgram quantities of protein utilizing the principle of protein-dye binding. Anal. Biochem. 1976;72:248–254.

Buranasinsup S, Sila-Asna M, Bunyaratvej N, Bunyaratvej A. In vitro osteogenesis from human skin-derived precursor cells. Dev Growth Differ. 2006;48:263–269.

Burger M. Altern und Krankheit., Leipzig, Georg Thieme 1947.

Burton DG, Matsubara H, Ikeda K. Pathophysiology of vascular calcification: Pivotal role of cellular senescence in vascular smooth muscle cells. Exp Gerontol. 2010;45:819-824.

Cristofalo VJ, Allen RG, Pignolo RJ, Martin BG, Beck JC. Relationship between donor age and the replicative lifespan of human cells in culture: a reevaluation Proc. Natl. Acad. Sci. U.S.A.1998;95:10614–10619

Croce MA, Sammarco R, Paolinelli Devincenzi C, et al. The skin equivalent model: developments and perspectives. Microscopie. 2004;2:31-36.

Endo T. Molecular mechanisms of skeletal muscle development, regeneration, and osteogenic conversion. Bone. 2015;80:2-13.

Giachelli CM, Speer MY, Li X, Rajachar RM, Yang H. Regulation of vascular calcification: roles of phosphate and osteopontin. Circ Res. 2005;96:717-722.

Hakim FT, Cranley R, Brown KS, Eanes ED, Harne L, Oppenheim JJ. Hereditary joint disorder in progressive ankylosis (ank/ank) mice. I. Association of calcium hydroxyapatite deposition with inflammatory arthropathy. Arthritis Rheum. 1984;27:1411-1420.

Ho AM, Johnson MD, Kingsley DM. Role of the mouse ank gene in control of tissue calcification and arthritis. Science. 2000;289:265–270.

Johnson K, Vaingankar S, Chen Y, et al. Differential mechanisms of inorganic pyrophosphate production by plasma cell membrane glycoprotein-1 and B10 in chondrocytes. Arthritis Rheum. 1999;42:1986-1997.

Kirsch T. Biomineralization--an active or passive process? Connect Tissue Res. 2012;53:438-445.

Kurz DJ, Decary S, Hong Y, Erusalimski JD. Senescence-associated β-galactosidase reflects an increase in lysosomal mass during replicative ageing of human endothelial cells. J Cell Sci. 2000;113:3613–3622.

Liu J, Xu K, Chase M, Ji Y, Logan JK, Buchsbaum RJ. Tiam1-regulated osteopontin in senescent fibroblasts contributes to the migration and invasion of associated epithelial cells. J Cell Sci. 2012;125:376-386.

Lomashvili KA, Cobbs S, Hennigar RA, Hardcastle KI, O'Neill WC. Phosphate-induced vascular calcification: role of pyrophosphate and osteopontin. J Am Soc Nephrol. 2004;15:1392-1401.

Mackenzie NC, MacRae VE. The role of cellular senescence during vascular calcification: a key paradigm in aging research. Curr Aging Sci. 2011;4:128-136.

Maier AB, Westendorp RG, van Heemst D. Beta-galactosidase activity as a biomarker of replicative senescence during the course of human fibroblast cultures. Ann N Y Acad Sci. 2007;1100:323-332.

Martin GM, Sprague CA, Epstein CJ Replicative life-span of cultivated human cells. Effects of donor's age, tissue, and genotype. Lab. Invest. 1970;23:86–92.

Mendes SC, Tibbe JM, Veenhof M, et al. Relation between in vitro and in vivo osteogenic potential of cultured human bone marrow stromal cells. J Mater Sci Mater Med. 2004;15:1123–1128.

Millán JL. Alkaline Phosphatases: Structure, substrate specificity and functional relatedness to other members of a large superfamily of enzymes. Purinergic Signal. 2006;2:335-341.

Pazolli, E., Luo, X., Brehm, S., et al. Senescent stromal-derived osteopontin promotes preneoplastic cell growth. Cancer Res. 2009;69:1230-1239.

Quaglino D, Boraldi F, Barbieri D, Croce A, Tiozzo R, Pasquali-Ronchetti I. Abnormal phenotype of in vitro dermal fibroblasts from patients with Pseudoxanthoma elasticum (PXE). Biochim. Biophys. Acta. 2000;1501:51–62.

Robert L, Labat-Robert J, Robert AM. Physiology of skin aging. Pathol Biol (Paris). 2009;57:336-341.

Rodrigues TL, Foster BL, Silverio KG, et al. Correction of hypophosphatasia-associated mineralization deficiencies in vitro by phosphate/pyrophosphate modulation in periodontal ligament cells. J Periodontol. 2012;83:653-663.

Ronchetti I, Boraldi F, Annovi G, Cianciulli P, Quaglino D. Fibroblast involvement in soft connective tissue calcification. Front Genet. 2013;5:4-22.

Selye H. Calciphylaxis. Editore: Chicago : University of Chicago Press, 1962.

Shanahan CM. Mechanisms of vascular calcification in CKD-evidence for premature ageing? Nat Rev Nephrol. 2013;9:661-670.

Shao JS, Cheng SL, Sadhu J, Towler DA. Inflammation and the osteogenic regulation of vascular calcification: a review and perspective. Hypertension. 2010;55:579-592.

Siddiqui NS, Altorok N. Image in clinical medicine. Diffuse Soft-Tissue Calcinosis. N Engl J Med. 2015;373:173.

Terkeltaub R, Rosenbach M, Fong F, Goding J. Causal link between nucleotide pyrophosphohydrolase overactivity and increased intracellular inorganic pyrophosphate generation demonstrated by transfection of cultured fibroblasts and osteoblasts with plasma cell membrane glycoprotein-1. Relevance to calcium pyrophosphate dihydrate deposition disease. Arthritis Rheum. 1994;37:934-941.

van der Loo B, Fenton MJ, Erusalimsky JD. Cytochemical detection of a senescence-associated beta-galactosidase in endothelial and smooth muscle cells from human and rabbit blood vessels. Exp Cell Res. 1998;241:309-315.

Wada T, McKee MD, Stietz S, Giachelli CM. Calcification of vascular smooth muscle cell cultures: inhibition by osteopontin. Circ Res. 1999;84:1–6.

nHDF   aHDF

A   B

Low CPD

2 μm   2 μm

C   D

High CPD

2 μm   2 μm

E   nHDF   aHDF

         5CPD 40 CPD   38 CPD
                        64 CPD   48 CPD
              5CPD

Fluorescence intensity   Fluorescence intensity

F   □ nHDF ▨ aHDF
                           ***
                    ***   ***
              ***   *** ○○
                          ○○
        ○○

     5   40 64   5   38 48
              CPD

Low CPD   High CPD

nHDF

aHDF

A   Low CPD   High CPD   B

10 days

20 days

30 days

% Calcified area

Low CPD
High CPD

100
80
60
40
20
4
2
0

10 d   20 d   30 d   10 d   20 d   30 d

	L CPD 10 d	L CPD 20 d	L CPD 30 d	H CPD 10 d	H CPD 20 d	H CPD 30 d
L CPD 10 d			*	*	*	**
L CPD 20 d			*		*	**
L CPD 30 d				*		**
H CPD 10 d					*	**
H CPD 20 d						
H CPD 30 d						

A

	Low CPD	High CPD
10 days		
20 days		
30 days		

B

Low CPD
High CPD

% Calcified area

100
80
60
40
20
2
0

10 d 20 d 30 d   10 d 20 d 30 d

	L CPD 10 d	L CPD 20 d	L CPD 30 d	H CPD 10 d	H CPD 20 d	H CPD 30 d
L CPD 10 d		**	***		***	***
L CPD 20 d			**		***	***
L CPD 30 d				***	***	***
H CPD 10 d					***	***
H CPD 20 d						
H CPD 30 d						

A

Culture condition	Time	nHDF	
		Low CPD	High CPD
DMEM		0.523±0.08	0.122±0.01
CM	10 d	0.947±0.06	0.685±0.02
	20 d	0.989±0.03	1.026±0.08
	30 d	1.049±0.03	1.276±0.09

	L CPD DMEM	L CPD 10 d	L CPD 20 d	L CPD 30 d	H CPD DMEM	H CPD 10 d	H CPD 20 d	H CPD 30 d
L CPD DMEM		**	**	***	**		***	***
L CPD 10 d					***			*
L CPD 20 d					***			
L CPD 30 d					***			
H CPD DMEM						***	***	***
H CPD 10 d							*	***
H CPD 20 d								
H CPD 30 d								

B

Culture condition	Time	aHDF	
		Low CPD	High CPD
DMEM		0.044±0.01	0.077±0.01
CM	10 d	0.612±0.15	2.936±0.03
	20 d	2.666±0.05	10.952±0.02
	30 d	2.823±0.27	6.969±0.21

	L CPD DMEM	L CPD 10 d	L CPD 20 d	L CPD 30 d	H CPD DMEM	H CPD 10 d	H CPD 20 d	H CPD 30 d
L CPD DMEM			***	***		***	***	***
L CPD 10 d			***	***		***	***	***
L CPD 20 d					***		***	***
L CPD 30 d					***		***	***
H CPD DMEM						***	***	***
H CPD 10 d							***	***
H CPD 20 d								***
H CPD 30 d								

ANKH				
Culture condition/Time		nHDF		aHDF	
		Low CPD	High CPD	Low CPD	High CPD
DMEM		**1,0**	1,2	0,6	1,3
CM	10 d	0.8	1,1	0,6	1,3
	20 d	0.9	1.2	0,5	1,7
	30 d	1.1	1.2	0,6	2,1

ENPP1				
Culture condition/Time		nHDF		aHDF	
		Low CPD	High CPD	Low CPD	High CPD
DMEM		**1,0**	2,3	0,5	0,4
CM	10 d	2,3	2,4	1,0	
	20 d	2,5	2,4	1,5	1,2
	30 d	2,2	2,4	1,7	1,9

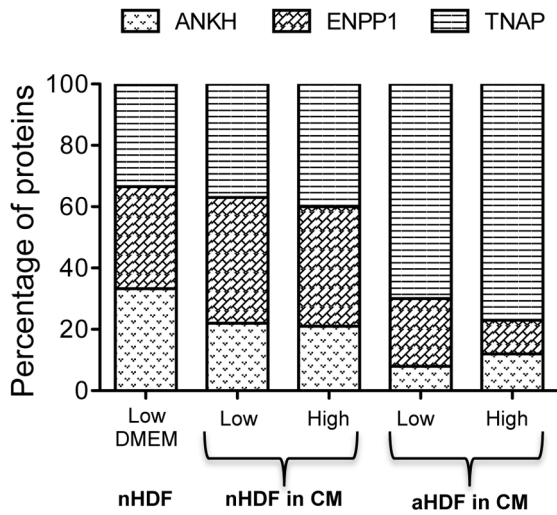| OPN				
Culture condition/Time		nHDF		aHDF	
		Low CPD	High CPD	Low CPD	High CPD
DMEM		**1,0**	1,8	1,2	2,1
CM	10 d	1,1	1,9	1,5	2,5
	20 d	1,1	2	1,2	2,4
	30 d	0,9	1,9	1,3	2,4

Table 1. Influence of *ex-vivo* (nHDF *vs* aHDF cultured in CM at low CPD) and *in-vitro* (low CPD *vs* high CPD in the same cell line cultured in CM) ageing on calcification-related parameters

Parameters	Ageing	
	Ex-vivo	*In-vitro*
Mineral deposition	✓	✓
TNAP activity	✓	only in aHDF
ANKH expression	✓	only in aHDF
ENPP1 expression	✓	--
ANKH+ENPP1/TNAP	✓	only in aHDF
OPN expression	--	✓